Available online at www.sciencedirect.com
ScienceDirect
Polymer 47 (2006) 6414–6421
polymer
www.elsevier.com/locate/polymer

Crystallization and phase transformation kinetics of poly(1-butene)/MWCNT nanocomposites

Santosh D. Wanjale, Jyoti P. Jog*

Polymer Science and Engineering Division, National Chemical Laboratory, Dr. Homi Bhabha Road, Pashan, Pune, Maharashtra 411008, India

Received 2 December 2005; received in revised form 3 July 2006; accepted 5 July 2006
Available online 28 July 2006

Abstract

Poly(1-butene)/MWCNT nanocomposites were prepared by simple melt processing technique. Crystallization, crystal-to-crystal phase transformation and spherulitic morphology were studied using differential scanning calorimetry (DSC), wide angle X-ray diffraction (WAXD) and optical microscopy (OM). The non-isothermal crystallization exhibited higher values of Z_t derived from Avrami theory and lower values of $F(T)$ obtained from Avrami–Ozawa analysis, while the isothermal crystallization revealed a significant increase in crystallization temperatures and lower crystallization half times compared to pristine PB. The observed changes in the crystallization kinetics were ascribed to the enhanced nucleation of PB in the presence of MWCNT. The nucleating activity calculated from the non-isothermal crystallization data revealed that the MWCNTs provide an active surface for the nucleation of PB. The optical micrographs exhibited significantly smaller crystallites with disordered morphology for the nanocomposites compared to the well defined spherulitic morphology for pristine PB. The rate of phase transformation from kinetically favored tetragonal to thermodynamically stable hexagonal form was noticeably enhanced as evidenced by the reduction in the half time for phase transformation from 58 h to 25 h for PB reinforced with 7% MWCNT.

Keywords: Poly(1-butene); MWCNT; Phase transformation

1. Introduction

PB is one of the members of the polyolefin family with excellent resistance to creep and environmental cracking [1]. From scientific point of view, the crystallization of PB is of great interest because of its spontaneous kinetically favored phase transformation in solid state. It is reported that the kinetics of phase transformation is influenced by pressure [2], temperature [3] and mechanical deformation [4]. This transformation and the structure development have been studied extensively by using differential scanning calorimetry, X-ray diffraction and IR spectroscopy [5–8]. Many researchers have tried different methods for enhancing the rate of phase transformation by blending with PP, addition of solid additives and nucleating agents, cold rolling and orientation [9–11]. Depending on the helical conformation and chain packing, PB crystallizes in four different polymorphic forms. After melting, PB crystallizes in the tetragonal crystal Form II with 11_3 helix and then it transforms into stable twined hexagonal crystal Form I of 3_1 helix. Form I generally melts at 130–138 °C, whereas, Form II melts at a low temperature of around 110–115 °C [4]. The third form having orthorhombic unit cell with 4_1 helix, can be obtained by precipitating the polymer from various solvents and generally melts at about 100 °C [4]. The fourth Form is I′ with untwined hexagonal form of 3_1 helical structure and melts at around 90–100 °C [4]. There have been few reports on the study of phase transformation in PB, at different temperature ranges as well as the effect of the presence of various solvents [11,12]. It has been reported that the rate of phase transformation is maximum at room temperature (25 °C) [11].

The reinforcement of fillers to the polymer matrix for improving the desired material properties has been studied intensively in the past and the incorporation of the inorganic phase

* Corresponding author. Tel.: +91 20 25902176; fax: +91 20 25902618.
E-mail address: jp.jog@ncl.res.in (J.P. Jog).

0032-3861/$ - see front matter © 2006 Elsevier Ltd. All rights reserved.
doi:10.1016/j.polymer.2006.07.011

is known to influence the crystallization kinetics, crystalline morphology, crystallite size and degree of crystallinity of polymers. Use of the nano size fillers for improvement in the properties is being explored and the effect of nanofillers such as layered silicates, nanotubes and nanoparticles on the crystallization behavior of polymers is a subject of interest [13,14]. In our previous studies [15,16] the nanocomposites of PB with organically modified clay has shown improved mechanical properties as well as enhanced rate of phase transformation. In this article, we present the preparation and characterization of PB/MWCNT nanocomposites with special emphasis on the effect of MWCNT on the crystallization and the most imperative tetragonal to hexagonal solid-state phase transformation.

2. Experimental

2.1. Materials and preparation of PB/MWCNT nanocomposites

Poly(1-butene) with molecular weight of 570,000 g/mol and multiwalled carbon nanotubes (MWCNTs) (with an internal diameter of 5–10 nm, outer diameter of 10–20 nm, length 0.5–200 μm and of 95% purity) were purchased from Aldrich Chemicals.

Melt mixing was carried out in Haake Polylab batch mixer of 50 g capacity at 60 rpm for 7 min at 150 °C. Three different compositions were prepared containing 3, 5 and 7 wt% MWCNTs and the nanocomposite samples were coded as PB3C, PB5C and PB7C, respectively. The samples were compression molded in to films having a uniform thickness of approximately 0.5 mm using a Carver hydraulic press (Model F-15181).

2.2. Crystallization study using differential scanning calorimetry

Non-isothermal and isothermal crystallization was studied by using a Perkin Elmer DSC-2 with TADS, in nitrogen atmosphere. The energy and temperature scales were calibrated using Indium as standard. Non-isothermal crystallization was studied for different cooling rates. The sample was heated at 10 °C/min up to 150 °C and held for 2 min to ensure complete melting and then crystallization peaks were recorded at different cooling rates. In isothermal crystallization, the sample was heated at 40 °C/min up to 150 °C and held for 2 min, then quenched at a cooling rate of 160 °C/min to the desired crystallization temperature (T_c) and the isothermal peak was recorded. The crystallization rate constant and the crystallization half time were determined by analyzing the isothermal crystallization peaks using Avrami equation [17].

2.3. Study of phase transformation kinetics using DSC and XRD

The phase transformation of PB and nanocomposites was studied using a Perkin Elmer DSC-7. The samples about 5–6 mg were prepared by melting the polymer and nanocomposites in the DSC cell at a rate of 10 °C/min up to 150 °C and held for 2 min and then cooled to room temperature at 40 °C/min. This step was carried out to ensure identical thermal history for each sample and then the samples were stored at room temperature. Since the two crystal forms exhibit melting points at about 128 and 114 °C for Form I and Form II, respectively, the phase transformation of Form II to Form I was monitored by measuring the crystallinities of two melting peaks corresponding to the two crystal forms at various time intervals. The kinetics of phase transformation of PB and PB/MWCNT nanocomposites was then analyzed by using Avrami theory.

The wide angle X-ray diffraction (WAXD) analysis was carried out for phase transformation studies using Rigaku X-ray diffractometer model Dmax 2500 with Cu Kα ($\lambda = 0.154$ nm) radiation operated at 40 kV and 100 mA. The samples were scanned in the 2θ range from 2 to 25° at various time intervals.

2.4. Optical microscopy

The spherulitic morphology of PB and PB/MWCNT nanocomposites was studied with a Leica Laborlux 12 Pol S polarized light microscope. The samples were prepared by melt pressing at 160 °C between a glass slide and a cover slip and kept for a minute to ensure uniform melting. The slide was then transferred to the hot stage maintained at 85 °C. The photomicrographs were taken under cross polarizers with a Canon Powershot S 50 digital camera.

3. Results and discussion

3.1. Non-isothermal crystallization study

Non-isothermal crystallization behavior of PB and the nanocomposites with MWCNT was studied to investigate the effect of various cooling rates and the MWCNT content. Different cooling rates of 2.5, 5, 10 and 20 °C/min were used. The crystallization temperatures for PB and PB/MWCNT nanocomposites at different cooling rates are shown in Table 1. It can be seen from Table 1, that the crystallization peak temperature (T_p) for both PB as well as for PB/MWCNT nanocomposites shifted to lower temperatures as the cooling rate was increased. However, it was observed that at a given cooling rate, the crystallization peak temperature (T_p) of PB/MWCNT nanocomposites was always higher than that of pristine PB and it shifted to higher temperature as the percentage of MWCNT increased. This clearly suggested that incorporation of MWCNT results in the heterogeneous nucleation for the PB matrix.

3.1.1. Non-isothermal crystallization kinetics

The isothermal crystallization process has been very well explained by the Avrami theory [17] and it can be also used for non-isothermal crystallization. For isothermal crystallization Avrami equation was given as follows:

Table 1
Non-isothermal crystallization parameters for PB and PB/MWCNT nanocomposites

Sample	ϕ (°C/min)	$t_{1/2}$ (min)	T_p (°C)	n	Z_t	Z_c
PB	2.5	1.5	79.4	4.2	4.99×10^{-3}	0.1201
	5	1.1	74.3	4.5	5.28×10^{-2}	0.5554
	10	1.0	69.8	4.6	0.54	0.9400
	20	0.9	62.9	4.2	3.48	1.0644
PB3C	2.5	1.4	91.8	3.7	1.38×10^{-2}	0.1807
	5	1.0	87.5	4.4	0.156	0.6894
	10	0.9	83.6	4.4	1.328	1.0288
	20	0.9	76.7	3.8	9.055	1.1165
PB5C	2.5	1.4	92.8	4.8	9.77×10^{-3}	0.1570
	5	1.0	88.9	4.6	0.1022	0.6337
	10	0.9	84.6	4.1	1.557	1.0453
	20	0.9	77.7	3.6	8.596	1.1136
PB7C	2.5	1.3	92.8	4.7	0.02	0.1888
	5	1.0	89.6	4.8	0.08	0.6117
	10	0.9	84.9	4.6	1.07	1.0070
	20	0.8	79.3	4.1	7.75	1.1078

ϕ = Cooling rate (°C/min); $t_{1/2}$ = crystallization half time (min); T_p = crystallization peak temperature (°C); n = Avrami exponent; Z_t = rate constant; Z_c = corrected rate constant for different cooling rates.

$$1 - X_t = \exp(-Z_t t^n) \tag{1}$$

The crystallization rate constant Z_t was corrected for the non-isothermal crystallization kinetics, by converting the temperature scale into time scale as follows:

$$\log Z_c = \frac{\log Z_t}{\phi} \tag{2}$$

The non-isothermal crystallization parameters determined using Avrami equation are presented in Table 1. The values of Z_t were found to increase with the increase in the cooling rates for both PB and PB/MWCNT nanocomposites, while the values of $t_{1/2}$ were found to decrease as the cooling rate increased. The values of Z_t for the nanocomposites were found higher than that for pristine PB. The rate constant 'Z_t', was corrected for the kinetic effect of various degrees of non-isothermal cooling denoted as Z_c and was found to increase with respect to cooling rate suggesting higher crystallization rates for the nanocomposites. The higher values of Z_c and the lower values of $t_{1/2}$ for the nanocomposites as compared to pristine PB imply that the carbon nanotubes enhance the crystallization of PB in PB/MWCNT nanocomposites.

A combined Avrami and Ozawa equation [18] was also used for analyzing the non-isothermal crystallization kinetics of PB and the PB/MWCNT nanocomposites.

$$\log Z_t + n \log t = \log K(T) - m \log \phi \tag{3}$$

which can be converted to

$$\log \phi = \log F(T) - a \log t \tag{4}$$

where $F(T) = [K(T)/Z_t]^{1/m}$ and 'a' is the ratio between the Avrami and Ozawa exponents i.e. n/m. $F(T)$ refers to the value of the cooling rate chosen at unit crystallization time, when the system has a defined degree of crystallinity.

Table 2
$F(T)$ and 'a' values for PB and PB/MWCNT nanocomposites

Sample	X_t (%)	$F(T)$	'a'
PB	20	8.04	1.33
	40	10.33	1.31
	60	12.23	1.31
	80	14.68	1.34
PB3C	20	6.08	1.20
	40	7.64	1.24
	60	9.06	1.23
	80	10.74	1.24
PB5C	20	5.81	1.23
	40	7.4	1.26
	60	8.77	1.29
	80	10.51	1.34
PB7C	20	6.06	1.43
	40	7.86	1.44
	60	9.32	1.45
	80	11.52	1.51

X_t = relative degree of crystallinity (%); $F(T)$ = kinetic parameter; 'a' = Avrami–Ozawa exponent (ratio of Avrami to Ozawa exponent).

At a given crystallinity, plots of $\log \phi$ vs $\log t$ gave straight lines with $\log F(T)$ as the intercept and '$-a$' as the slope. Table 2 presents the values of $F(T)$ and 'a' calculated from the graphs. The values of Avrami–Ozawa exponent 'a' were 1.3 and about 1.4 for all the cooling rates for PB and PB7C nanocomposites, respectively. It can be seen that the $F(T)$ values for PB and the nanocomposites increased with increase in the relative degree of crystallization, suggesting that the time required for reaching the finite degree of crystallization increased with respect to cooling rate. However, lower values of $F(T)$ for the nanocomposites clearly suggest that the time required for reaching the defined degree of crystallization was lower in case of nanocomposites as compared to the time required for the same degree of crystallization for pristine PB. These results can be ascribed to the accelerated crystallization of PB in the presence of MWCNTs.

3.1.2. Nucleating activity

The nucleating activity of the MWCNT was determined by using the method described by Dobreva and Gutzow [19], where the cooling rate and the degree of supercooling are taken into consideration. For homogeneous nucleation the following equation was used:

$$\log \phi = A - \frac{B}{2.303\ \Delta T_p^2} \tag{5}$$

For the heterogeneous system in which the foreign particles help in crystallization, the following equation was used:

$$\log \phi = A - \frac{B^*}{2.303\ \Delta T_p^2} \tag{6}$$

where ϕ is the cooling rate, ΔT_p is the degree of supercooling ($T_m - T_p$), A, B and B^* are constants.

The nucleation activity (Φ), is defined as the ratio of B^* to B and is determined from the slopes of linear plots of $\log \phi$ vs $1/\Delta T_p^2$ (Fig. 1). It has been stated that for active surfaces

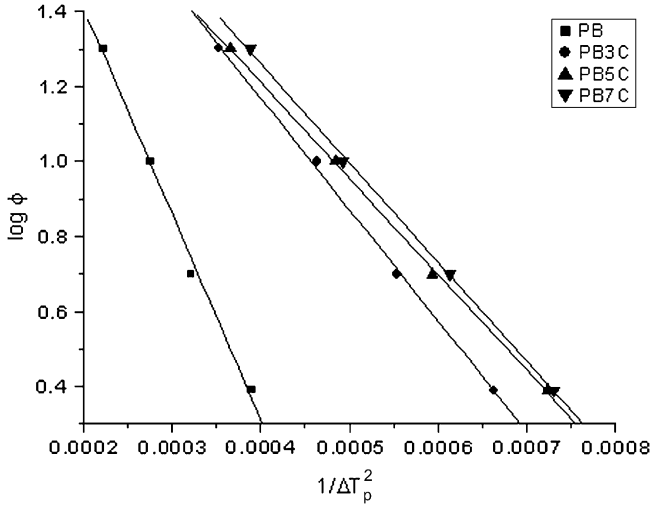

Fig. 1. $\log \phi$ vs $1/\Delta T_p^2$ for PB and PB/MWCNT nanocomposites.

Φ tends to zero whereas, if it tends to one, the surface is considered as an inert surface for nucleation [20]. The nucleating activity was found to be 0.54, 0.47 and 0.48, for PB3C, PB5C and PB7C nanocomposites, respectively. These values suggest that the MWCNTs provide an active surface for crystallization. It is worth noting here that the nucleation activity of PB/clay nanocomposites was found to be about 0.897 [21]. This clearly suggested the nucleating ability of the nanotubes is much higher compared to that of organically modified clay.

3.2. Isothermal crystallization study

Isothermal crystallization was studied for PB and PB/MWCNT nanocomposites in the temperature range of 72–86 °C and 86–96 °C for PB and PB/MWCNT nanocomposites, respectively. The crystallization curves were analyzed using Avrami equation to determine the crystallization parameters. Fig. 2 illustrates the variation of crystallization half time, $t_{1/2}$ with crystallization temperature, T_c. As can be seen from the figure, $t_{1/2}$ increased with increasing T_c for PB as well as PB/MWCNT nanocomposites while the nanocomposites were crystallized at higher temperature than those for PB. It can be seen that at comparable temperatures of crystallization, the $t_{1/2}$ for the nanocomposites was much lower than those observed for pristine PB. For example, the crystallization half time ($t_{1/2}$) for PB at 86 °C was 121 s while it reduced to 18 s for 7% nanocomposite. The Avrami exponent was found in between 1.8 and 2.2 for both PB and PB/MWCNT nanocomposites. The values of rate constant k at 86 °C for PB and PB7C were 1.03×10^{-4} and 2.84×10^{-3}, respectively. The increase in the rate constant implies acceleration in crystallization of PB in the presence of MWCNT.

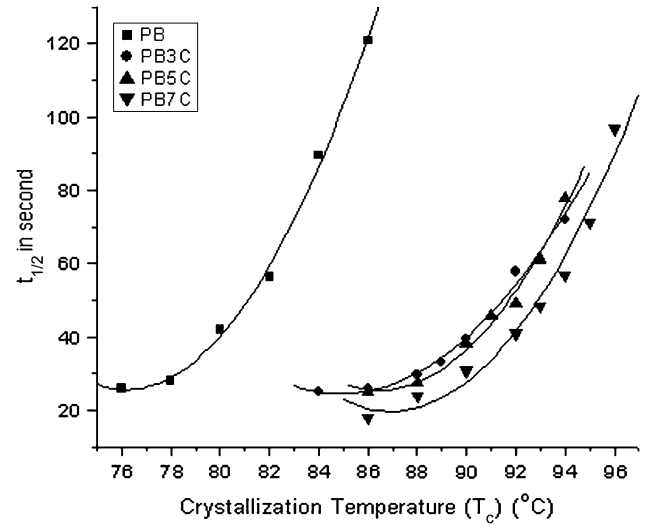

Fig. 2. Crystallization half time ($t_{1/2}$) for PB and PB/MWCNT nanocomposites.

Isothermal crystallization kinetics was further analyzed using the spherulitic growth rate in the context of the Lauritzen–Hoffman secondary nucleation theory [22]. The growth rate G is given as a function of the crystallization temperature T_c, using following bi-exponential equation:

$$G = G_0 \exp\left[\frac{-U^*}{R(T_c - T_\infty)}\right] \exp\left[\frac{-K_g}{T_c \Delta T f}\right] \tag{7}$$

where G_0 is the pre-exponential factor, the first exponential term contains the contribution of diffusion process to the growth rate, while the second exponential term is the contribution of nucleation process. U^* and T_∞ are the Vogel–Fulcher–Tamman–Hesse (VFTH) parameters describing the transport of molecular segments across the liquid/crystal interphase to the crystallization surface, K_g is the nucleation constant, ΔT denotes the degree of supercooling ($T_m - T_c$) and f is the correction factor. The left hand side of equation when plotted against $1/T_c \Delta T$ gave a straight line having a slope equal to K_g. For the growth rate G the approximation: $G = 1/t_{1/2}$ can be used. For a secondary or heterogeneous nucleation, K_g can be calculated from

$$K_g = \frac{nb\sigma\sigma_e T_m^0}{\Delta H_f k \beta} \tag{8}$$

where σ and σ_e are the side surface and fold surface free energies, respectively, which measure the work required to create a new surface, b is the distance between the two adjacent fold planes, β is the parameter that depends on the crystallization regime and k is the Boltzmann constant.

Fig. 3 showed the graph from Lauritzen–Hoffman equation and the K_g values were determined from the slopes of the lines for PB and PB/MWCNT nanocomposites. The K_g value for PB was 4.3×10^5 and it decreased to 2.9×10^5, 2.5×10^5 and 3.1×10^5 for PB3C, PB5C and PB7C nanocomposites, respectively. It is well known that a foreign surface frequently reduces the nucleus size needed for the crystal growth as the creation of the interface between polymer crystal and substrate may be less hindered than the creation of the corresponding free polymer crystal surface. A heterogeneous nucleation path makes the use of a foreign pre-existing surface to reduce the free energy opposing primary nucleation because of which

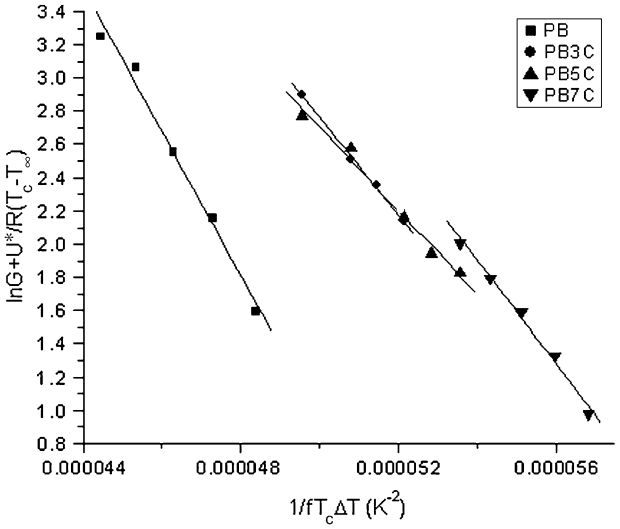

Fig. 3. $\ln G + U^*/R\ (T_c - T_\infty)$ vs $1/f\ T_c \Delta T$ for PB and PB/MWCNT nanocomposites.

the K_g decreases as the amount of filler increased. The lower values of K_g obtained in the present study thus was ascribed to the heterogeneous nucleation of PB in the nanocomposites.

The energy of activation (E_a) was calculated from the slopes of the graph [$1/n \ln k$ vs $1/T_c$] for isothermal crystallization [23]. The slopes were found to be 20.5, 18.0, 17.9, and 21.9 for PB, PB3C, PB5C and PB7C, respectively, while the E_a was found to be about 170 kJ/mol for PB and 149.6, 148.7 and 182 kJ/mol for PB3C, PB5C and PB7C, respectively. The marginal increase in the activation energy for PB7C was ascribed to the hindered mobility of polymer chains due to the presence of MWCNT.

The non-isothermal crystallization studies confirm the nucleating activity of MWCNT and higher crystallization rate of PB in the nanocomposites. The isothermal crystallization results also support these findings as evidenced by the increase in crystallization temperature, lower crystallization half times and nucleation constant (K_g). The observed increase in the overall crystallization rate could be attributed to the enhanced nucleation of PB due to reinforcement of MWCNT.

3.3. Phase transformation study using DSC and XRD

There have been few reports on the effect of additives and nucleating agents on the crystallization and phase transformation of PB. According to Zhang et al. [9] E3B, calcium carbonate–pimelic acid mixture was effective in accelerating the isothermal crystallization as well as the rate of phase transformation. Kaszonyiova et al. [11] reported that the addition of sodium salicylate increased the rate of crystallization and the addition of talc reduced the rate of crystallization, and also showed that the solid additives had no effect on the phase transformation. Hong and Spruiell [10] studied the effect of cold rolling, orientation and additives. Beatty and Rogers [24] tried to increase the tie fibrils population by controlling crystallization process while Choi and White [25] reported

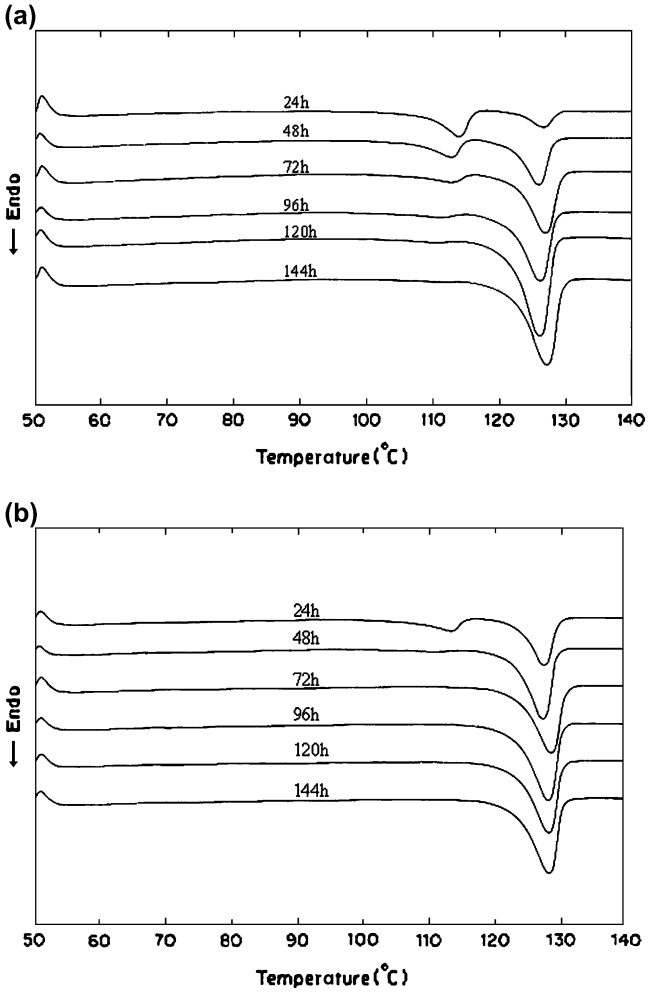

Fig. 4. (a) DSC curves illustrating phase transformation of PB at various time intervals. (b) DSC curves illustrating phase transformation of PB7C at various time intervals.

that the filaments having higher level of crystalline orientation showed higher rate of phase transformation.

We have studied the phase transformation of PB and PB/MWCNT nanocomposites at room temperature by measuring the crystallinity of the two forms at various time intervals. The DSC heating scans for PB and PB7C at various time intervals are shown in Fig. 4a and b, respectively. From the figure it was revealed that as the aging time increases, the area under the lower temperature peak (114 °C, Form II) decreases and the area under the higher temperature peak (128 °C, Form I) increases.

The crystallinities for each form was calculated by taking the ratio of the heat of fusion observed to the heat of fusion reported for 100% crystalline forms. The reported values of heat of fusion for 100% crystalline forms, i.e. Form I (125.4 J/g), and for Form II (75.2 J/g) were used [26]. Comparing the values of crystallinities of Form I and Form II of PB one can examine the effectiveness of the MWCNT on the phase transformation at various aging time intervals. Table 3 presents the values of crystallinities for PB and PB/MWCNT nanocomposites. A remarkable increase in the crystallinity of

Table 3
Percentage crystallinities of Form I and Form II at different time intervals for PB and PB/MWCNT nanocomposites

Time (h)	PB		PB3C		PB5C		PB7C	
	X_I	X_{II}	X_I	X_{II}	X_I	X_{II}	X_I	X_{II}
24	8.4	28.1	20.4	23.3	17.9	24.2	28.1	16.7
48	22.0	18.2	36.8	10.3	37.8	7.7	47.7	2.4
72	33.3	9.5	47.5	2.7	50.1	1.6	51.2	0.5
96	39.1	3.8	51.3	0.9	53.5	0.4	52.2	–
120	46.5	1.0	52.6	0.5	54.3	–	53.5	–
144	48.2	0.3	54.5	0.2	54.3	–	55.1	–

X_I = percentage crystallinity of Form I; X_{II} = percentage crystallinity of Form II.

Form I was observed in the case of nanocomposites for all the aging time intervals. The higher crystallinity values of Form I suggest that the MWCNTs promote the crystal transformation through nucleation of Form I directly from amorphous phase and these results are in good agreement with those reported by Hong and Spruiell [10]. The percent conversion of Form I was obtained from the crystallinities at different time intervals (The crystallinity of the sample, which was completely converted to Form I was taken as reference.). After 48 h the conversion of Form I for PB was 40.4% while it was 64%, 66%, and 82.9% for PB3C, PB5C and PB7C nanocomposites, respectively. The half time for phase transformation (50% conversion to Form I) was calculated using percent conversion and was about 58 h for PB while in case of PB/MWCNT nanocomposites the half time significantly reduced to 35, 36 and 25 h for PB3C, PB5C and PB7C, respectively. The remarkable reduction in the half time for the phase transformation in PB nanocomposites indicates the enhanced rate of phase transformation in the presence of MWCNT.

The higher values of crystallinity of the PB/MWCNT nanocomposites compared to pristine PB suggest lower amorphous content and it is well known that in the process of Form II to Form I phase transformation a slight extension of chain segment occurs. The observed increase in the transformation rate could be explained on the basis of the favorable (chain) extension due to the additional stress acting on the molecular chains through the crystal amorphous interphase required for the formation of Form I. This is to be noted here that the increase in the rate of phase transformation with decrease in amorphous fraction was observed by Azzurri et al. [27]. Gohil et al. [28] also suggested that the additional tensile stress induced due to the tightening of the tie molecules on the chain segments through the crystal amorphous interphase facilitates the local extension of the 11_3 helix to 3_1 helical conformation and enhances the nuclei formation which results in the higher rate of phase transformation. The crystallinity of the nanocomposites was found to be almost same for all the compositions, however, the transformation from Form II to Form I was found to increase with the content of MWCNTs. This suggests that the lowering in amorphous fraction is not the only factor in enhancing the rate of phase transformation. One of the other reasons for improvement in the rate could be the disordered crystallite of Form II [29]. To see the effect of MWCNTs on the morphology of the spherulites, optical microscopic studies were carried out. Fig. 5a and b shows the optical micrographs of PB and PB3C, respectively. As can be seen from the figure that the pristine PB shows well defined spherulitic morphology, but in case of PB3C very small crystalline structures are observed. The micrographs clearly indicate that the dispersion of MWCNT in the polymer matrix hinders the formation of ordered crystallites of Form II and does not allow enough time to attain the inherent morphology of the spherulite of the pristine polymer due heterogeneous nucleation. Thus, the presence of disordered Form II crystallites in the nanocomposites also contributes to the observed enhancement of the phase transformation rate.

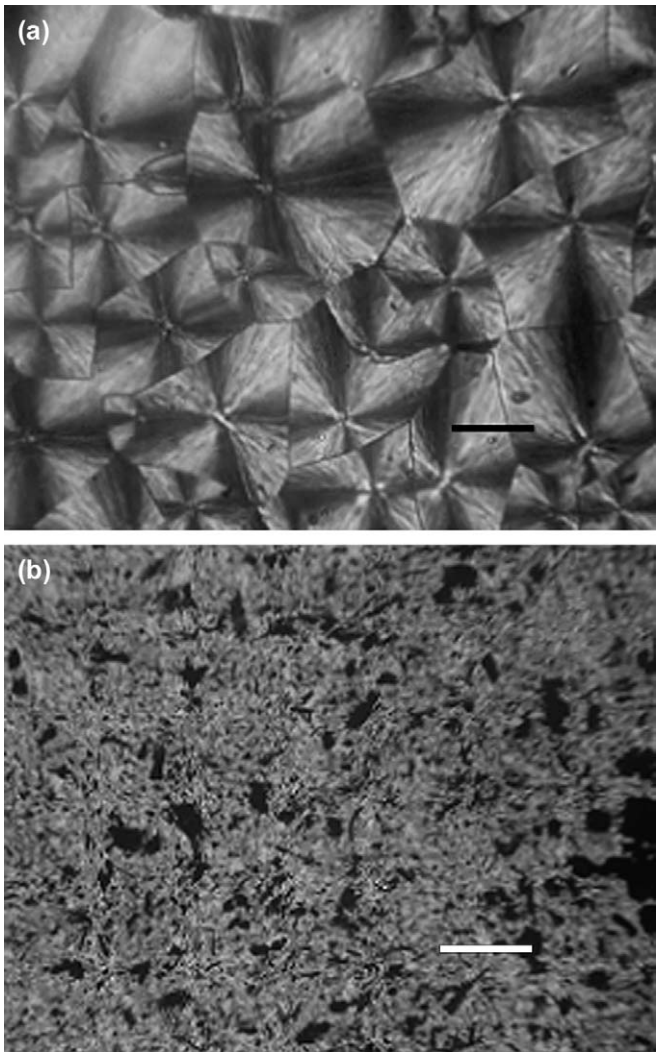

Fig. 5. (a) Optical micrograph of PB (magnification 100×, scale bar 1 cm = 100 μm). (b) Optical micrograph of PB3C (magnification 100×, scale bar 1 cm = 100 μm).

The Avrami theory was used to study the phase transformation kinetics and the plots are shown in Fig. 6. The rate constant for phase transformation was found to be 1.81×10^{-3} for PB and it increased with the MWCNT content in case of nanocomposites. The rate constant was about 0.042 in case of PB7C suggesting an increase in rate of phase

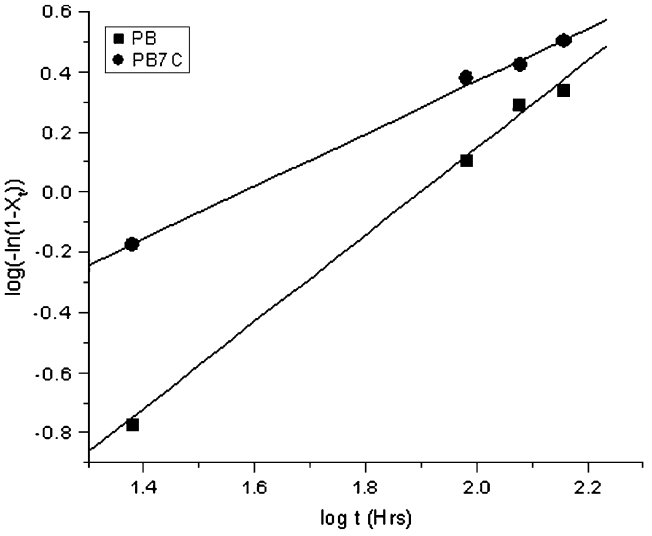

Fig. 6. $\log(-\ln(1-X_t))$ vs $\log t$ for PB and PB7C.

transformation. The Avrami exponent for PB was found to be 1.44. The values of the Avrami exponent for PB are in good agreement with the reported values [9]. The Avrami exponent for the PB/MWCNT was found to be 0.87. The fact that the Avrami exponent is different for the pristine polymer and the PB/MWCNT nanocomposite clearly indicates that the basic mechanism of phase transformation is altered in the presence of MWCNT and also suggests that the process of nucleation and growth of Form I is different for PB/MWCNT nanocomposites.

The phase transformation of PB and PB7C nanocomposites was also studied using WAXD. The two crystalline forms exhibit peaks characteristic to each form. For Form I, the X-ray diffraction peaks are observed at 2θ values of 10.0, 17.6, and 21.6° corresponding to planes (110), (300) and (211), respectively, whereas the peaks at 2θ values of 12, 17, 18.5° corresponding to planes (200), (220) and (213), respectively for Form II. The film samples were initially melted and then allowed to cool to room temperature and the X-ray diffraction patterns were recorded at different predetermined time intervals. Fig. 7A and B illustrates the WAXD patterns of PB and PB7C recorded at various time intervals. A series of diffraction patterns were recorded in which the intensity of peak at 12° for Form II was monitored. Fig. 8 shows the intensity ratio (I_t/I_0), where I_t is the intensity at time t and I_0 is the intensity at time t is zero. It has been observed that as the aging time increased, the ratio was found to decrease and the magnitude of decrement of ratio for PB7C was found to be larger compared to pristine PB for all the time intervals studied. These results suggest the enhanced rate of phase transformation in case of nanocomposites.

Similar increase in the rate of crystallization and the rate of phase transformation has been reported in our previous study of PB nanocomposites with organically modified clays [15]. However, the rate of crystallization as well as the rate of phase transformation was found to be higher for PB/MWCNT nanocomposites than that of PB/clay nanocomposites. In the

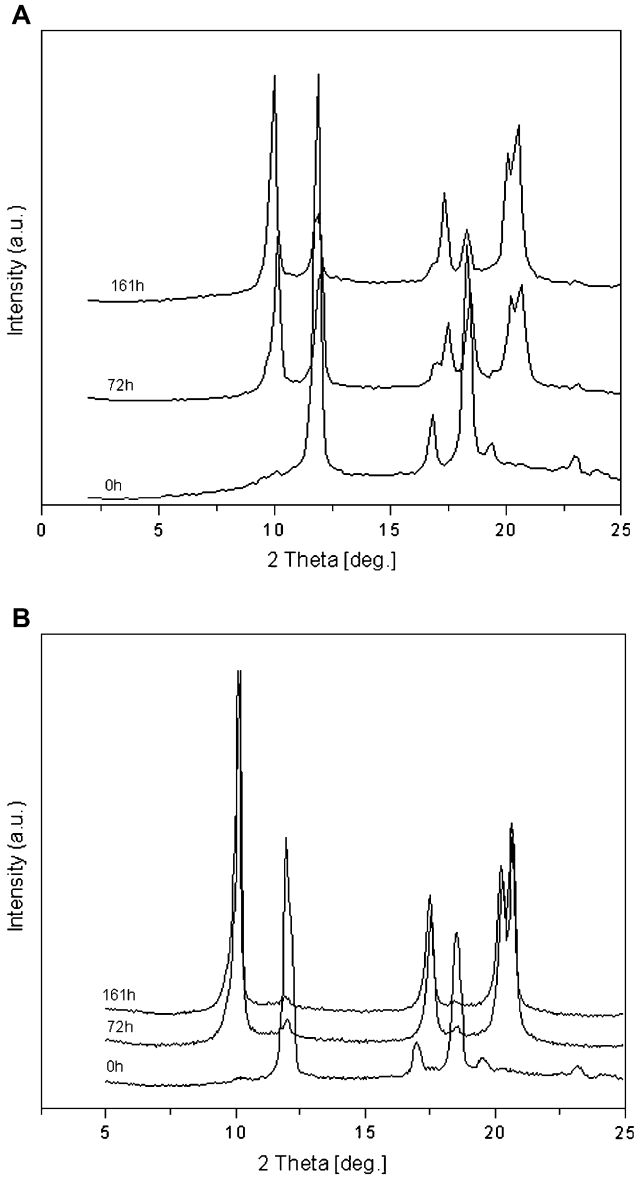

Fig. 7. (A) WAXD patterns for PB at different time intervals. (B) WAXD patterns for PB7C at different time intervals.

present case, the observed increase in the rate of phase transformation thus could be ascribed to the heterogeneous nucleation of PB leading to small defective crystals of Form II and to the possibility of the crystal transformation through the enhanced nucleation of Form I directly from the amorphous phase. It is also to be noted here that, in view of the reported literature, the addition of MWCNT to PB not only results in enhanced nucleation but also the rate of phase transformation.

4. Conclusions

The significant observations of the present investigation can be summarized as follows. The non-isothermal crystallization studies revealed the higher values for Z_t and lower values for $F(T)$ compared to pristine PB suggesting the enhanced

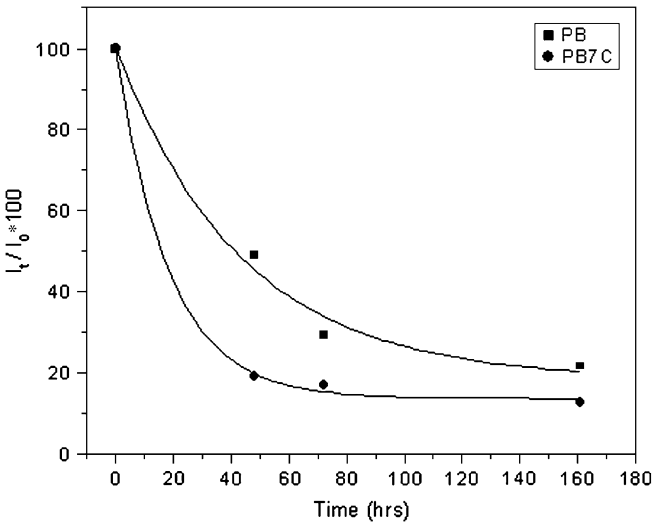

Fig. 8. Change in peak intensity (percent) of peak at 12° of Form II at different time intervals.

crystallization rate in the presence of MWCNT. The nucleation activity of MWCNT obtained from non-isothermal crystallization was found to be 0.48 for PB7C nanocomposite, which entails the highly active surface for nucleation. In isothermal crystallization studies, the crystallization half time was found significantly lower and the crystallization temperature was increased by 15 °C, while the nucleation constant (K_g) deduced from Lauritzen–Hoffmann equation was found lower compared to PB, corroborating the active nucleation of PB due to incorporation of MWCNT. The results of XRD studies exhibited enhanced rate of phase transformation for nanocomposites and were consistent with the DSC results. The optical micrographs exhibited significantly smaller crystallites of disordered morphology for the nanocomposites as compared to the well-defined spherulitic morphology for pristine PB. Avrami analysis of phase transformation revealed higher rate for PB/MWCNT nanocomposites while the Avrami exponent was found to be lower for PB/MWCNT nanocomposites compared to pristine PB. These results suggest that the mechanism for nucleation and growth of Form I was altered in the presence of MWCNT. The observed increase in the rate of phase transformation for the nanocomposites was attributed to the decrease in the amorphous content and to the enhanced nucleation of Form I due to disordered crystallite morphology. Since the crystal-to-crystal phase transformation plays an imperative role in improving the physical and mechanical properties of PB, these results demonstrate that the use of MWCNT offers a novel route to enhance the transformation as the time required for the 50% conversion of Form I was found to be significantly reduced.

Acknowledgement

SDW would like to thank Council of Scientific and Industrial Research (CSIR), New Delhi, India, for providing Senior Research Fellowship.

References

[1] Marigo A, Marega C, Cecchin G, Collina G, Ferrara G. Eur Polym J 2000;36:131–6.
[2] Nakafuku C, Miyaki T. Polymer 1983;24:141–8.
[3] Tanaka A, Sugimoto N, Asada T, Onogi S. Polym J 1975;7:529–37.
[4] Nakamura K, Aoike T, Usaka K, Kanamoto T. Macromolecules 1999; 32:4975–82.
[5] Fu Q, Heck B, Strobl G, Thomann Y. Macromolecules 2001;34: 2502–11.
[6] Samon JM, Schultz JM, Hsiao BS, Wu J, Khot S. J Polym Sci Polym Phys 2000;38:1872–82.
[7] Hsu CC, Geil PH. J Macromol Sci Phys 1986;B25:433–66.
[8] Armeniades C, Baer E. J Macromol Sci 1967;B1:309–34.
[9] Zhang X, Zhang X, Shi G. Thermochim Acta 1992;205:245–52.
[10] Hong K, Spruiell J. J Appl Polym Sci 1985;30:3163–88.
[11] Kaszonyiova M, Rybnikar F, Geil PH. J Macromol Sci Phys 2004; B43:1095–114.
[12] Kaszonyiova M, Rybnikar F, Geil PH. J Macromol Sci Phys 2005; B44:377–96.
[13] Krikorian V, Pochan D. Macromolecules 2004;37:6480–91.
[14] Wiemann K, Kaminsky W, Gojny F, Schulte K. Macromol Chem Phys 2005;206:1472–8.
[15] Wanjale SD, Jog JP. J Macromol Sci Phys 2003;42B:1141–52.
[16] Wanjale SD, Jog JP. J Polym Sci Polym Phys 2003;41:1014–21.
[17] Avrami MA. J Chem Phys 1940;8:212–24.
[18] Ozawa T. Polymer 1971;12:150–8.
[19] Dobreva A, Gutzow I. J Non-Cryst Solids 1993;162:13–25.
[20] Kim SH, Ahn SH, Hirai T. Polymer 2003;44:5625–34.
[21] Wanjale SD, Jog JP. Private communication.
[22] Hoffman JD, Davis GT, Lauritzen SI. In: Hannay NB, editor. Treatise on solid state chemistry, vol. 3. New York: Plenum; 1976 [chapter 7].
[23] Wu TM, Liu CY. Polymer 2005;46:5621–9.
[24] Beatty C, Rogers C. Polym Prepr (Am Chem Soc Div Polym Chem) 1977;18:641–8.
[25] Choi C, White JL. Polym Eng Sci 2001;41:933–9.
[26] Cimmino S, Lorenzo ML, Pace E, Silvestre C. J Appl Polym Sci 1998;67:1369–81.
[27] Azzurri F, Flores A, Alfonso G, Calleja B. Macromolecules 2002;35: 9069–73.
[28] Gohil R, Miles M, Petermann J. J Macromol Sci Phys 1982;21B: 189–201.
[29] Azzurri F, Alfonso G, Gomez M, Marti M, Ellis G, Marco C. Macromolecules 2004;37:3755–62.